Modeling of internal wave impact on hypothetical pillars of hydraulic engineering constructions in the conditions of the Sakhalin island shelf

EKATERINA ROUVINSKAYA[1], OXANA KURKINA[1], ANDREY KURKIN[1],
ANDREY ZAYTSEV[2]
[1]Laboratory of Modeling of Natural and Anthropogenic Disasters
Nizhny Novgorod State Technical University n.a. R.E. Alekseev
603950 Nizhny Novgorod, Minin St., 24
RUSSIAN FEDERATION
[2]Special Research Bureau for Automation of Marine Researches,
Far Eastern Branch of Russian Academy of Sciences,
693013 Yuzhno-Sakhalinsk, Gorky Street, 25
RUSSIAN FEDERATION
oksana.kurkina@mail.ru, e.rouvinskaya@gmail.com, aakurkin@gmail.com, http://www.nntu.ru

Abstract: The velocity field induced by nonlinear internal waves generated by multicomponent barotropic tidal flow over topography for the conditions of the Sea of Okhotsk (South-East shelf of Sakhalin Island) is used to estimate dynamical loads on underwater vertical cylindrical parts of marine engineering structures. The intensity of lateral surface pressure and the rate inertia moment are expressed according to Morison's formula for a cylidrical pile of 2.5 m diameter and 100 m height and computed as functions of time. They can reach values of $1.9 \cdot 10^5$ N and 10 MN·m, respectively, during the flood phase of the tide.

Key-Words: Internal waves, drag force, inertial force, shear force, torque, load, Morison equation, near-bottom velocity, barotropic tide

1 Introduction

Investigation of internal gravity waves is one of the most important problems of modern oceanology. Such waves propagate within the stably stratified ocean, exerting a significant influence on all the processes taking place in the surrounding environment. Although the internal and surface gravity wave are of the same nature, the amplitudes of the former are much larger, since the reduced gravity acceleration acts on the fluid particles within the fluid. Intensive internal gravity waves are one of the most serious threats that call into question the safety of hydraulic engineering constructions on the continental shelf [1, 2].

The velocities induced by internal waves can produce significant local loads and bending moments [3 – 8] on the cantilever beams supporting a drilling rig and oil platforms. There are cases when, under the influence of internal waves, the oil platforms are displaced 200 m in the horizontal and 10 m in the vertical direction. Nonlinear internal waves can cause a significant increase (up to twice) in the tension of the anchor chains [5] used in spar platforms. The intensity of influence of such a wave with a maximum horizontal velocity of 2.1 m/s is comparable with the influence of a surface wave with a length of about 300 m and a height of 18 m [9]. The results of field observations in the South China Sea suggest that intensive internal waves induce significantly greater loads and torques in hydraulic engineering constructions than surface waves. The danger of such waves is recognized as critical, so development and adaptation of models that allow to estimate a risk of the intense internal waves impact on hydraulic engineering constructions is an actual and practically significant task.

When underwater structures are flowed around by stream induced by internal gravity waves, the intensity of the the side surface pressure on hydraulic engineering constructions is usually calculated approximately according to the Morison equation [10 – 12]. In the framework of this approach flow pressure contains the inertial (linear, depending on the acceleration of fluid particles in the wave) and the velocity (non-linear resistance force, quadratic in velocity) components. This method for the first time was suggested in [13] to evaluate the forces associated with surface waves and influencing on vertical cylindrical objects in water, supports, piles or pillars, supposing that the cylinder diameter, D, is much smaller than the typical wavelength L so that the wave field almost doesn't "feel" the pillar. Let us consider in more details the application of this method to estimate the

impact of internal waves on the support of hydraulic engineering constructions.

2 Mathematical model of internal wave impact on hypothetical pillars of hydraulic engineering constructions

Following [14], we consider small oscillations in the vertical plane (x, z) of a cylinder submerged into water (Fig. 1).

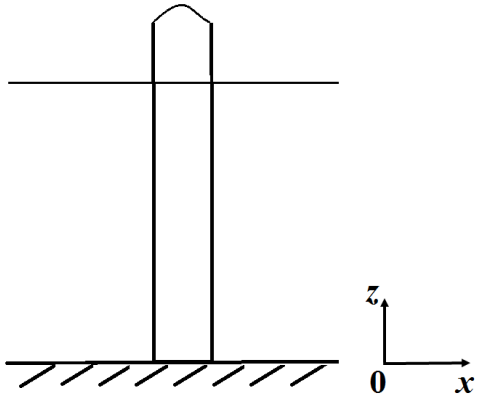

Fig. 1. A cylinder submerged into water

It is assumed that the distribution of masses inside the cylinder can be generally inhomogeneous. The equations of motion of the cylinder are:

$$m\frac{d^2x_c}{dt^2} = X\,,\ m\frac{d^2z_c}{dt^2} = Z\,,\ J\frac{d^2\varphi}{dt^2} = M\,, \quad (1)$$

where m – mass of the cylinder, J – the moment of inertia with respect to cylinder's center of gravity, x_c, z_c, φ – coordinates of the center of gravity and the rotation angle of the cylinder centerline, X, Z – the projections of the external forces and M – their moment relative to the center of gravity. When we calculate the values of X, Z, M, associated with the water pressure under the influence of flow around the cylinder, we assume that the pressure is exerted only by the normal component of the flow, v_n, w_n. The intensity $f_n(s)$ of pressure on the lateral surface of cylinder is calculated by the Morison formula [10 – 12] and contains inertial f_I and velocity f_D components.

$$\begin{aligned} f_n(s,t) &= f_I + f_D\,,\\ f_I(t) &= \rho g S C_M a_n\,,\\ f_D(t) &= \rho g R C_D \,|\, v_n^e \,|\, v_n^e\,, \end{aligned} \quad (2)$$

where s is coordinate along the cylinder axis, $s = 0$ corresponds to the center of mass of the cylinder,

$$v_n^e = v_n - v_n^c\,,\ v_n = u(s,t)\cos\varphi + w(s,t)\sin\varphi\,,$$
$$a_n = \frac{dv_n}{dt}\,,\ v_n^c = \frac{dx_c}{dt}\cos\varphi + \frac{dz_c}{dt}\sin\varphi + s\frac{d\varphi}{dt}\,.$$

Here v^e_n – relative normal projection of the velocity at point s on the cylinder centerline, v_n and a_n — projections of the velocity and acceleration of water, $u(s, t)$ and $w(s, t)$ calculated at the point $x = x_c + s\sin\varphi$, $z = z_c + s\cos\varphi$, v^c_n – projection of the velocity of the cylinder centerline's point s, $S = \pi R^2$ – cross-sectional area, R – radius of the cylinder, constants C_D and C_M are empirical, averaged over the typical period of the wave drag and inertia coefficients, respectively. They can be defined for a wide range of control parameters: the Kelegan – Carpenter number K (= U_mT/D), the Reynolds number Re (= U_mD/ν) and the relative roughness k/D, where D is the diameter of the circular cylinder, U_m is maximum flow velocity, T is the typical period of oscillations in the flow, ν is the kinematic viscosity, k is the average size of the irregularities.

The force F_n directed by the normal to the cylinder axis and the moment M' are obtained by integrating over the length of the underwater part of the cylinder

$$F_n(t) = \int_{s_1}^{s_0} f_n(s)ds\,,\ M'(t) = \int_{s_1}^{s_0} f_n(s)sds\,, \quad (3)$$

where $s_1 < 0$ corresponds to the lower end of the cylinder, and $s_0 > 0$ is the point of intersection the cylinder axis and the sea surface. If the cylinder (pile, support) is assumed to be stiff (the bending angles are small) and is fixed at the bottom, then $s \cong z$, and the integration in (3) can be carried out over the entire water column in case when the cylinder is longer than the sea depth, and over the entire height of the cylinder when it is completely submerged.

The force F_n and the moment M' can be easily determined if the velocity, normal to the cylinder, and acceleration components are known. In the case of small oscillations, this is the horizontal velocity component u and its time derivative – an acceleration $a_n = \partial u/\partial t$, which can be easily calculated.

To compute the integrals (3), the normal velocity and acceleration must be known for the whole range of values of the vertical coordinate z, which is not always possible for experimental data and field observations, or the resolution can be inadequate. Therefore, preliminary theoretical estimates play here a very important role. Integration can be done using the Simpson method, with the help of standard utilities.

It should be noted that the representation of the flow pressure force on the cylinder (2) at the point in the form of a sum of two components f_I and f_D is valid only approximately. Such a separation is

semiempirical and requires in each case an experimental proof. It is not uniform in all possible ranges of *K*, *Re* and *k/D*. More general formulations for forces acting on a solid submerged in a fluid body were presented by Lighthill [15] in terms of both velocity and vorticity. It was shown that the viscous drag force and the inviscid inertia force are not independent, and that the appearance and diffusion of vorticity influences on both components of the force in a nonstationary flow. In this case, even the coefficient of inertia (or the coefficient of the added mass), C_M, is not constant and varies in time, even during the oscillation period of the flow, and also when the control parameters (*Re*, *K*, *k*/*D*, shape and orientation of the body) are changing. However, this simplified approach is useful for the first rough estimates of dynamical loads from wave-induced currents on underwater engineering structures.

3 Numerical modeling of internal gravity wave dynamics in the conditions of the Sakhalin island shelf

The main goal of this work is to study the influence of internal gravity waves on the pillars of hydraulic engineering constructions. The following tasks were solved for this purpose:

– initialization of the background conditions in the numerical model: temperature, salinity, pressure, water level fluctuations, bathymetry data were processed (data records were made by SakhNIRO, Russia in the summer in the southern part of the Sakhalin continental slope in 1999 – 2003 years);

– modeling of internal wave dynamics in oceanographic conditions that correspond to the shelf zone of Sakhalin Island in the Sea of Okhotsk;

– estimation of internal waves' impact on hypothetical pillars of hydraulic engineering constructions on the basis of the predicted velocity fields induced by internal waves.

Investigation of internal waves' dynamics was carried out in the framework of program complex intended for numerical modeling of propagation and transformation of such waves in the ocean, that implements procedure of numerical integration of fully nonlinear two-dimensional (vertical plane) system of equations of hydrodynamics inviscid incompressible stratified fluid in the Boussinesq approximation bearing in mind the impact of barotropic tide [16]:

$$\vec{V}_t + (\vec{V}\nabla)\vec{V} - f\vec{V}\times\vec{k} = -\nabla P - \vec{k}\rho g\,, \qquad (4)$$

$$\rho_t + \vec{V}\nabla\rho = 0\,, \qquad (5)$$

$$\nabla\vec{V} = 0\,, \qquad (6)$$

$$\rho = \frac{\rho_f - \rho_0}{\rho_0}\,, \qquad (7)$$

where $\vec{V}(u, v, w)$ is the velocity vector, ∇ is the three dimensional vector gradient operator, subscript t denotes the time derivative, ρ_f – the density of sea water, ρ_0 – the average or characteristic density (introduced owing to the Boussinesq approximation that assumes that the density $\rho_f = \rho_0(1 + \rho)$ only changes insignificantly in the basin and ρ is a nondimensional quantity that has a meaning of density anomaly), P is the pressure, g is acceleration due to gravity, f is, as above, the Coriolis parameter and $\vec{k}$ is the unit vector along the z-direction. The waves propagate in the x-direction, y-axis is perpendicular to the wave motion and z is the depth.

The normal to the wave propagation (cross-section) velocity is included in the model, but no variation along the y-coordinate is allowed. This is realised by neglecting the partial derivatives with respect to y in the basically three-dimensional equations (4 – 7). The equations are transformed to a terrain-following coordinate system (so-called sigma-coordinates). The equations are solved over a domain bounded below by the topography $h(x)$ (prescribed by the user) and covered by a rigid lid at the surface.

To initialize the model, it is necessary to prescribe horizontally homogeneous density field of water masses $\rho_{mean}(z)$ as well as the velocity distribution in the barotropic tidal field in the computational domain. The steps of the numerical scheme in space and time are chosen to satisfy the Courant–Friedrich–Levy criterion for stability.

To determine water depth we used good resolution bathymetry data between 140 and 150 degrees west longitude and 40 and 50 degrees north latitude, that were provided by SakhNIIRO. Then we defined a section between points 143.55 *E*, 46.25 *N* and 144.13 *E*, 45.36 *N* in the shelf of Sakhalin Island area. Its length is 128 km. Since horizontally-homogeneous density field is used in our numerical model, the density profile from the outer edge of the section was taken, which is obtained by approximating and averaging of in-situ data on temperature, salinity and pressure from the sensors. Detailed description of algorithm of this stage is presented in [17]. Density anomaly field, bathymetry for chosen section and position of hypotetic pile are shown in Fig. 2.

An important condition for initialization of the model is the structure of the barotropic tide. The horizontal velocity u_{btr} in the barotropic tide is given by:

$$u_{\text{btr}} = \frac{H}{r(x)} \sum_i U_{\max_i} \sin(\sigma_i t + \varphi_i) = \\ = \sum_i \frac{Q_i}{r(x)} \sin(\sigma_i t + \varphi_i), \quad (8)$$

$$Q_i = U_{\max i} H, \quad (9)$$

$$U_{\max i} = \sqrt{\frac{g}{H}} \eta_i, \quad (10)$$

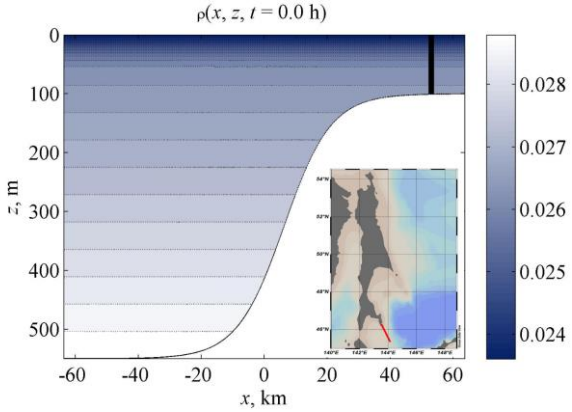

Fig. 2. Density anomaly field, bathymetry and position of hypotetic pile.

re Q_i – the maximum cross flux of water for the corresponding component of the tide, $r(x) = H – h(x)$ – the local depth of the fluid, σ_i – the frequency of the tidal component, φ – its initial phase, and the i-index indicates the various tidal components (M2, N2, etc.). The flow velocities of the components $U_{\max i}$ in the barotropic tide are calculated from the data on the tidal level rise η_i. From the continuity equation we obtain the expression for the vertical velocity of the barotropic tide

$$w_{\text{btr}} = \sum_i Q_i \frac{r'(x)}{r^2(x)} (z - H) \sin(\sigma_i t + \varphi_i). \quad (11)$$

The barotropic tide velocity v_{btr} in the transverse direction with respect to our section is given by:

$$v_{\text{btr}} = \sum_i \frac{fQ_i}{\sigma_i r(x)} \cos(\sigma_i t + \varphi_i). \quad (12)$$

In accordance with (8) – (12), the initial velocity field is initialized as follows (there are no internal waves at the initial time):

$$u = \sum_i \frac{Q_i}{r(x)} \sin(\varphi_i), \quad (13)$$

$$v = \sum_i \frac{fQ_i}{\sigma_i r(x)} \cos(\varphi_i), \quad (14)$$

$$w = \sum_i Q_i \frac{r'(x)}{r^2(x)} (z - H) \sin(\varphi_i). \quad (15)$$

The barotropic tide was initialized as a superposition of the components M2, N2, Q1, O1, P1, K1 [18].The Coriolis parameter in the considered sea area is $f = 0.0001051$ s^{-1}.

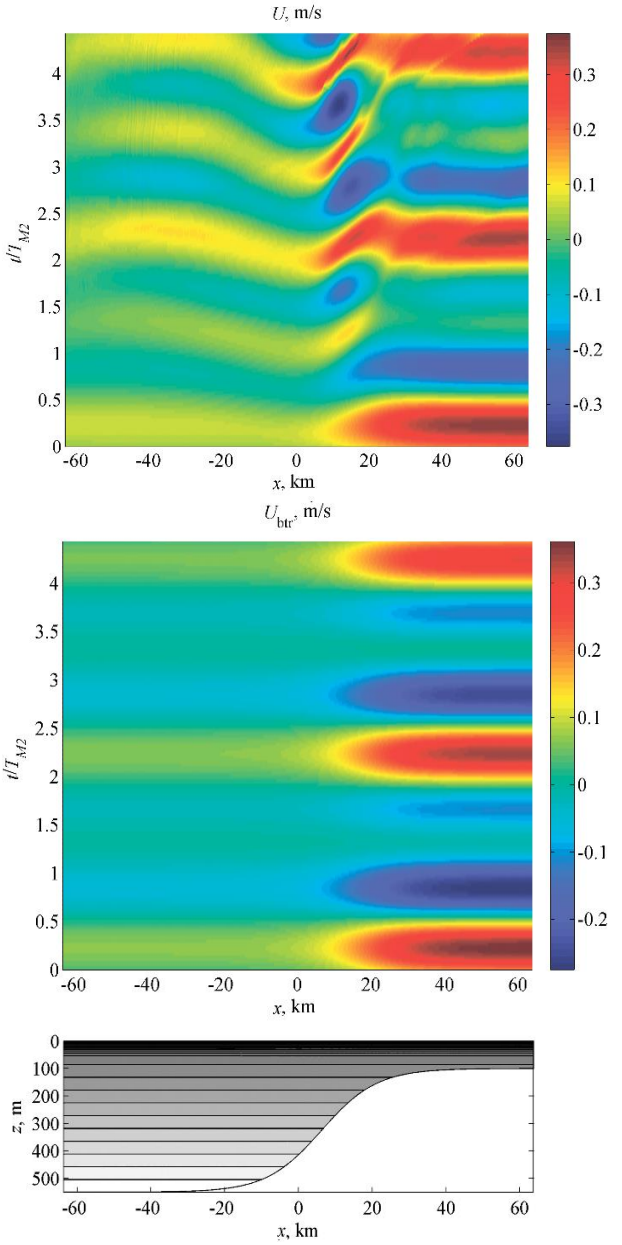

Fig. 3. *x-t* diagram of the total velocity in the projection on the tangent to the bottom line (upper panel) and the velocity of the barotropic tide (middle panel).

For engineering applications, it is of great interest to estimate the contribution of internal waves to the formation of near-bottom currents, so we have analyzed the structure of the tangential to the bottom velocities for this model case. We defined the projection of the total velocity on the tangent to the bottom and obtained its time dependence at each point of the cross-section (Fig. 3, Fig. 4). Also we plotted the *x-t* diagrams only for

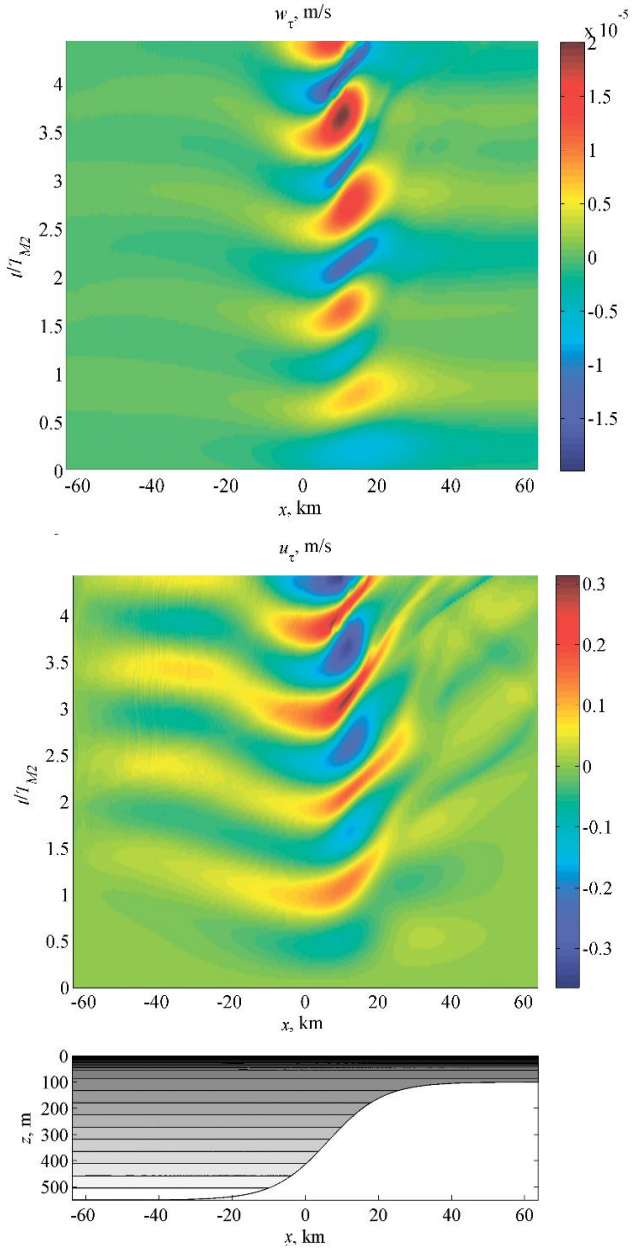

Fig. 4. *x-t* diagram of the vertical (upper panel) and horizontal (middle panel) baroclinic velocity components for chosen section

the velocities of the near-bottom barotropic tidal flows and determined the contribution of the vertical velocity components of the wave field to the total near-bottom velocity. As can be seen from Fig. 4, this contribution is negligible for our model case. Finally, let us separate out the contribution of internal waves to the velocities of the near-bottom currents. From Fig. 4 one can see that the values of the velocities of the bottom currents in the field of internal waves on the shelf edge (where the topography changes are mostly expressed) are of the same order as the velocities of the barotropic tidal current for the Sakhalin island shelf. But the internal wave components of the near-bottom velocities have a more complex, irregular spatio-temporal structure. However, structure of the current in the shallower part of the section is again determined mainly by the barotropic tidal flow.

To calculate shear forces and torques we determine the field of horizontal velocity (and acceleration) at the location of hypothetic pile (we put it to the point x = 55 km) throughout the depth of the fluid depending on time (Fig. 5). As one can see, the velocity field becomes more irregular after some time due to the generation of internal waves.

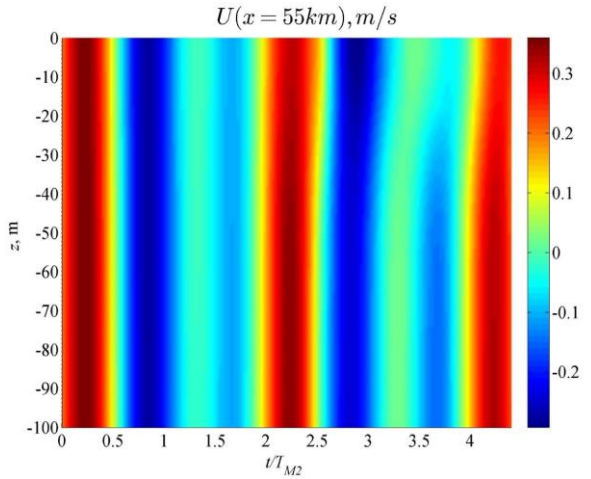

Fig. 5. The total velocity at the location of hypothetic pile throughout the depth of the fluid depending on time

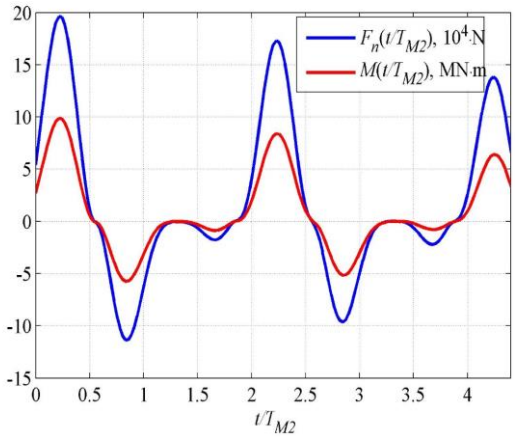

Fig. 6. The total force and the moment of force with respect to a bottom at the location of hypothetic pile depending on time

Total shear force and the moment M' with respect to a bottom (see eq. (3)) are shown in Fig. 6. The characteristic length of internal waves is of order of hundreds of meters, so that the effect of pile with R = 2.5 m to the wave field can be ignored (i.e., D/L < 0.15). We choose the empirical coefficients C_M = 1.8 and C_D = 0.6 taking into account the considerations presented in article [4]. The maximal absolute values of the force and the moment are

reached at the first tidal cycle while there are no intensive internal waves and the structure of the current is still approximately barotropic. When internal waves are generating, the velocity/acceleration may have different signs at different depths. Consider a distribution of the loads upon unit length of the pillar at different times (Fig. 7). In Morison equation, the force acting to a cylinder is a linear sum of a velocity-squared-dependent drag force and an acceleration-dependent inertial force. The inertial force is mainly smaller in absolute value than the drag force during this process (Fig. 8). But at certain times inertial force becomes comparable to drag force. Significant irregularity of the distribution of the load throughout the depth is the typical feature of the influence of internal waves.

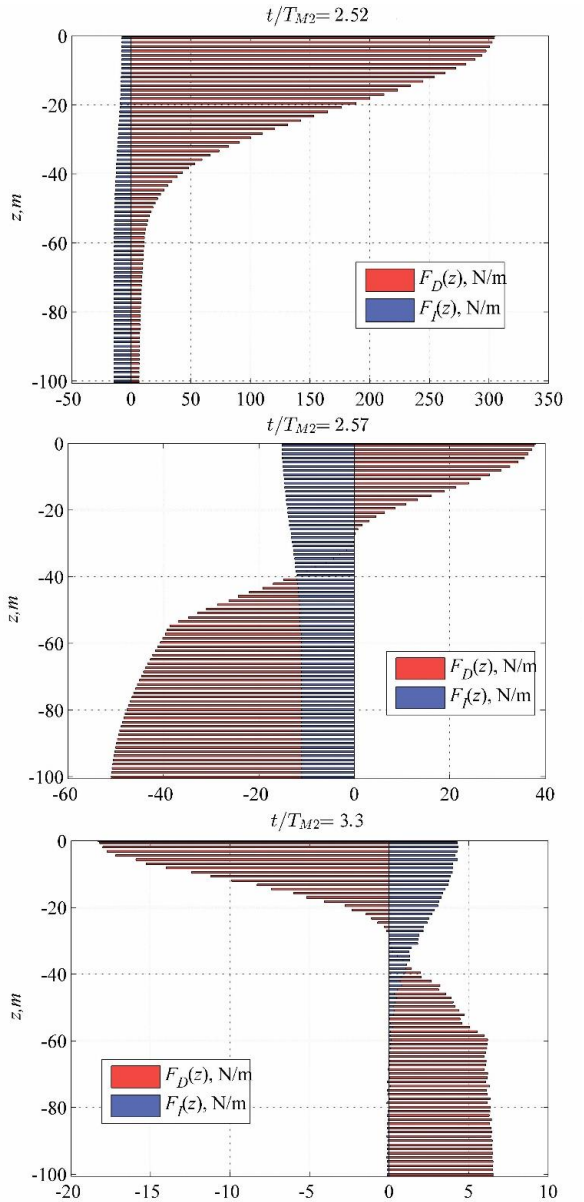

Fig. 7. The vertical distribution of the drag force and inertial force (both normalized for the unit length of the pile) at different times.

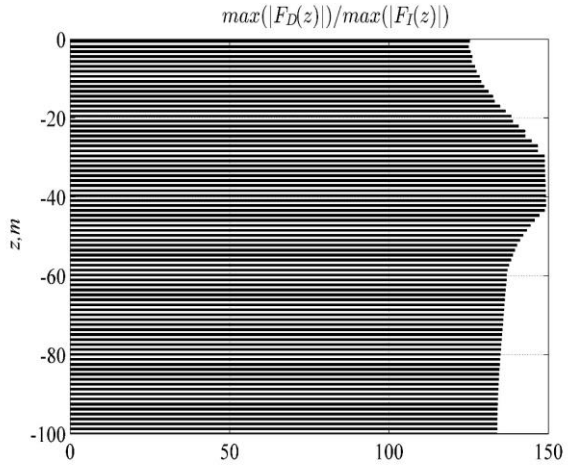

Fig. 8. The vertical distribution of the ratio of drag force maximal absolute value to inertial force maximal absolute value (both normalized for the unit length of the pile).

Acknowledgements

The results were obtained in the framework of the state task programme in the sphere of scientific activity of the Ministry of Education and Science of the Russian Federation (projects No. 5.4568.2017/6.7 and No. 5.1246.2017/4.6) and grants of the President of the Russian Federation (NSh-6637.2016.5 and SP-2311.2016.5).

References:

[1] Chakrabarti S. (Ed.) Handbook of offshore engineering. London: Elsevier, 2005.

[2] Osborne A.R. Nonlinear ocean waves and the Inverse Scattering Transform, San Diego: Elsevier, 2010.

[3] Cai S., Long X., Gan Z. A method to estimate the forces exerted by internal solitons on cylindrical piles, *Ocean Engineering*, 2003, Vol. 30, No. 5, pp. 673–689.

[4] Cai S., Long X., Wang S. Forces and torques exerted by internal solitons in shear flows on cylindrical piles, *Applied Ocean Research*, 2008, Vol. 30, No. 1, pp. 72–77.

[5] Song Z.J., Teng B., Gou Y., Lu L., Shi Z.M., Xiao Y., Qu Y. Comparisons of internal solitary wave and surface wave actions on marine structures and their responses, *Applied Ocean Research*, 2011, Vol. 33, No. 2, pp. 120-129.

[6] Si Z., Zhang Y., Fan Z. A numerical simulation of shear forces and torques exerted by large-amplitude internal solitary waves on a rigid pile in South China Sea, *Applied Ocean Research*, 2012, Vol. 37, pp. 127–132.

[7] Xie J., Jian Y., Yang L. Strongly nonlinear internal soliton load on a small vertical circular cylinder in two-layer fluids, *Applied Mathematical Modelling*, 2010, Vol. 34, No. 8, pp. 2089–2101.

[8] Xie J., Xu J., Cai S. A numerical study of the load on cylindrical piles exerted by internal solitary waves, *Journal of Fluids and Structures*, 2011, Vol. 27, No. 8, pp. 1252–1261.

[9] Du T., Sun L., Zhang Y., Bao X., Fang X. An estimation of internal soliton forces on a pile in the ocean, *J. Ocean Univ. China*, 2007, Vol. 6/2, pp. 101–116.

[10] Newman J.N. Marine Hydrodynamics. Cambridge: MIT Press, 1977.

[11] Aleshkov Yu.Z. The theory of the interaction of waves and obstacles. Leningrad: LST Publ., 1990, 371 p. (in Russian)

[12] Khalfin I.Sh. The impact of waves on the offshore oil and gas facilities. Moscow: Nedra, 1990. 313 p. (in Russian)

[13] Morison J.R., O'Brien M.P., Johnson J.W., Schaaf S.A. The forces exerted by surface waves on piles, *Petroleum transactions*, 1950, AIME 189, pp. 149-157.

[14] Tovstik P.E., Tovstik T.M., Shekhovtsov A.S. Shekhovtsov V.A. Motion of a flowing cylinder under waves, *Vestnik St.Petersburg Univ*., 2012, Series 1, No 3, pp. 137–143. (in Russian)

[15] Lighhill M.J. Fundamentals concerning wave loading on offshore structures, *Journal of Fluid Mechanics*, 1986, Vol. 173, pp. 667-681.

[16] Tyugin D.Yu., Kurkin A.A., Pelinovsky E.N., Kurkina O.E. Increase of productivity of software package for modeling of internal gravity waves IGW Research with the help of Intel® Parallel Studio XE 2013, *Fundamental and Applied hydrophysics*, 2012, Vol. 5, No. 3, pp. 89-95.

[17] Rouvinskaya E.A., Kurkina O.E., Kurkin A.A. Modeling of internal weather in the ecosystem of the stratified sea shelf, *Ecological Systems and Devices*, 2011, No. 6, pp. 8-16. (in Russian)

[18] Romanov A.A., Sedaeva O.S., Shevchenko G.V. Seasonal and tidal variations of the sea level between Hokkaido and Sakhalin Islands based on satellite altimetry and coastal tide gauge data, *J. Pacific Oceanography*, 2004, No. 2, pp. 117-125.